Hydrometallurgy 191 (2020) 105195

Contents lists available at ScienceDirect

Hydrometallurgy

journal homepage: www.elsevier.com/locate/hydromet

Optimization of sulfuric acid leaching of a Vietnamese rare earth concentrate

Nguyen Trong Hung[a], Le Ba Thuan[a], Tran Chi Thanh[b], Masayuki Watanabe[c], Hoang Nhuan[a], Do Van Khoai[c], Nguyen Thanh Thuy[a], Nguyen Van Tung[a], Noboru Aoyagi[c], Doan Thi Thu Tra[d], Nguyen Trung Minh[e], Manish Kumar Jha[f], Jin-Young Lee[g,*], Rajesh Kumar Jyothi[g,*]

[a] Institute for Technology of Radioactive and Rare Elements (ITRRE)-VINATOM-MOST, 48 Lang Ha, Dong Da, Hanoi, Viet Nam
[b] Vietnam Atomic Energy Institute (VINATOM)-Ministry of Science and Technology (MOST), 59 Ly Thuong Kiet, Hoan Kiem, Hanoi, Viet Nam
[c] Japan Atomic Energy Agency (JAEA), 2-4 Tokaimura, Nakagun, Ibaraki 319-1195, Japan
[d] Institute of Geological Sciences (IGS)-Vietnam Academy of Science and Technology (VAST), 84 Chua Lang, Dong Da, Hanoi, Viet Nam
[e] Vietnam National Museum of Nature (VNMN)-VAST, 18 Hoang Quoc Viet, Cau Giay, Hanoi, Viet Nam
[f] Metal Extraction and Recycling Division, CSIR-National Metallurgical Laboratory (NML), Jamshedpur 831007, India
[g] Convergence Research Center for Development of Mineral Resources (DMR), Korea Institute of Geoscience and Mineral Resources (KIGAM), Daejeon 34132, Republic of Korea

ARTICLE INFO

Keywords:
Rare earths
Yen Phu xenotime
Leaching
Modeling
Optimizing

ABSTRACT

The modeling of Yen Phu (Vietnam) xenotime concentrate leaching by sulfuric acid was studied for the purpose of optimizing the process. The response surface methodology (RSM) based on a central composite face-centered (CCF) design was empirically used to model the interactive effect of the independent variables, namely leaching temperatures of 250–450 °C, acid/concentrate (acid/conc.) mass ratios of 0.8–1.8, and leaching times of 2–6 h, on the dependent response, namely the leaching yield. And a CCF model for the leaching of the concentrate was proposed that exhibited good consistency with the experimental data. The shrinking core models for spherical particles of constant size based on the Arrhenius equation were empirically used to study the kinetics of the leaching. The activation energies calculated from the kinetic models for the chemical reaction and diffusion rate stages have the same value of 17.3 $kJ{\cdot}mol^{-1}$, which fitted well to a mixed control model of the chemical reaction followed by a diffusion stage at leaching temperatures in the range of 473–593 K. The kinetic studies of the leaching indicated that the leaching percent rate (or leaching yield) is controlled by the leaching temperature. The optimization of the leaching process was estimated by analyzing the contributions of the coefficients of the CCF model to the leaching yield. The results indicated that the effect of leaching temperature on leaching yield is the strongest; it is five times higher than that of the acid/conc. Mass ratio and four times higher than that of the leaching time. The effects of acid/concentration mass ratio and leaching time on leaching yield are insignificant. In addition, the optimum data for leaching are as follows: the leaching temperature, acid/conc. Mass ratio, and leaching time are 320 °C, 1.3, and 4 h, respectively. The proposed CCF model and kinetic study suggested that the optimization of the Yen Phu xenotime concentrate leaching is controlled by the leaching temperature; and the CCF model can potentially be applied in the commercial operation of Yen Phu xenotime concentrate leaching after pilot tests on 50 kg dry concentrate per batch.

1. Introduction

Rare earths (REs) are found in minerals such as monazite, bastnaesite, cerite, xenotime, gadolinite, fergusonite, allanite, and samarskite in commercially exploitable quantities. Only these three minerals contain a significant amount of REs: bastnaesite $(La,Ce)FCO_3$, monazite $(La,Ce,Y,Th)PO_4$, and xenotime YPO_4 (xenotime is the third most important source of REs). The former is rich in light REs (Lanthanum, Cerium, Praseodymium and Neodymium), and the two letters contain all the REs from Lanthanum to Lutetium and Yttrium (Jha et al., 2016; Gupta and Krishnamurthy, 2005; Jordens et al., 2013; Sadri et al., 2017a, 2017b; Xie et al., 2014; Kanazawa and Kamitani, 2006; Innocenzi et al., 2014; John et al., 2019). However, monazite is highly radioactive (Kumari et al., 2015; Zhu et al., 2015; Panda et al.,

* Corresponding authors.
E-mail addresses: jinlee@kigam.re.kr (J.-Y. Lee), rkumarphd@kigam.re.kr (R.K. Jyothi).

https://doi.org/10.1016/j.hydromet.2019.105195
Received 14 August 2018; Received in revised form 10 September 2019; Accepted 2 November 2019
Available online 06 November 2019
0304-386X/ © 2019 Elsevier B.V. All rights reserved.

2014); so, medium REs (samarium, europium and gadolinium) and heavy REs (terbium, dysprosium, holmium, erbium, thulium, ytterbium, lutetium and yttrium) have been extracted mainly from xenotime (Innocenzi et al., 2014; Pamela et al., 1998; Vijayalakshmi et al., 2001; Kuzmin et al., 2012; El Hady et al., 2016).

Various processing routes have been developed to recover REs. After mining and grinding, the ore is beneficiated by flotation, magnetic, or gravity methods to produce RE concentrates (Jordens et al., 2013) that subsequently undergo acid leaching or caustic cracking; the impurities are removed from the leachate to recover total RE oxides (TREO) or compounds (Jha et al., 2016; Gupta and Krishnamurthy, 2005; Sadri et al., 2017a, 2017b) that separate and purify the total RE oxides or compounds to obtain individual RE metals of high grade and commercial value (Jha et al., 2016; Xie et al., 2014).

There are two industrial methods for the leaching of xenotime, namely acid leaching (Jha et al., 2016; Gupta and Krishnamurthy, 2005; Pamela et al., 1998; Vijayalakshmi et al., 2001; Kuzmin et al., 2012; Vladimir et al., 2012; John et al., 2019) and caustic cracking (Jha et al., 2016; Gupta and Krishnamurthy, 2005; Sadri et al., 2017a, 2017b; Berry et al., 2017; Xu et al., 2012). The leaching of xenotime by the latter method requires an implementation under a pressure of several atmospheres; for example, in autoclave equipment, to obtain a high leaching yield (Jha et al., 2016; Gupta and Krishnamurthy, 2005; Kumari et al., 2015), thereby limiting the method for large-scale development. The former method, however, has been developed on an industrial scale in many countries (Jha et al., 2016; Gupta and Krishnamurthy, 2005; Pamela et al., 1998; Vijayalakshmi et al., 2001; Kuzmin et al., 2012; John et al., 2019).

Pyrometallurgy has also been widely used in the treatment process of high-grade RE concentrate, but this method is gradually losing its competitiveness in the treatment of low-grade RE concentrate owing to the difficulty of treating small amounts, its high energy consumption, and the many environmental pollutants and additional burdens associated with environmental treatment. Meanwhile, hydrometallurgy (leaching) is an effective technology for recovering REs from low-grade RE concentrate because it offers advantages that include selective leaching by appropriate solvents, low processing cost, and relatively low pollutant generation (Kim et al., 2014; Jha et al., 2016; Gupta and Krishnamurthy, 2005; Feng et al., 2013).

Technologies used in the leaching of xenotime in particular and RE minerals in general have been reviewed in detail by Jha et al. (2016), Kumari et al. (2015), Sadri et al. (2017a, 2017b), Innocenzi et al. (2014), and John et al. (2019). The acid leaching for xenotime breakdown involves attacking with concentrated (98%) sulfuric acid at 250–300 °C for several hours. The REs, iron (Fe), thorium (Th), and uranium (U) are converted to soluble sulfates during the sulfuric acid leaching. The major reaction includes (Jha et al., 2016; Gupta and Krishnamurthy, 2005):

$$2REPO_4 + 3H_2SO_4 \xrightarrow{t^o \sim 300^oC} RE_2(SO_4)_3 + 2H_3PO_4 \tag{1}$$

The major side reactions include (Jha et al., 2016; Gupta and Krishnamurthy, 2005):

$$2U_3O_8 + O_2 + 6H_2SO_4 \xrightarrow{t^o \sim 300^oC} 6UO_2SO_4 + 6H_2O\uparrow \tag{2}$$

$$ThO_2 + 2H_2SO_4 \xrightarrow{t^o \sim 300^oC} Th(SO_4)_2 + 2H_2O\uparrow \tag{3}$$

$$Fe_2O_3 + 3H_2SO_4 \xrightarrow{t^o \sim 300^oC} Fe_2(SO_4)_3 + 3H_2O\uparrow \tag{4}$$

$$Al_2O_3 + 3H_2SO_4 \xrightarrow{t^o \sim 300^oC} Al_2(SO_4)_3 + 3H_2O\uparrow \tag{5}$$

After the completion of the acid leaching process, almost all the REs are solubilized by water (Jha et al., 2016; Gupta and Krishnamurthy, 2005; John et al., 2019; Pamela et al., 1998; Vijayalakshmi et al., 2001; Wang et al., 2017; Sadri et al., 2017a, 2017b). The sulfate solution is purified to remove impurities before it can be taken for separation (Jha et al., 2016; Feng et al., 2013; Yoon et al., 2016). Generally, the acid/conc. Mass ratio lies between 1/1 and 2/1 dependence upon the grade of the RE mineral concentrate and the gangue minerals in the concentrate. Acid consumption will increase if the iron mineral content in the concentrate is high. In addition, acid consumption is affected by leaching temperature and time (Jha et al., 2016; Gupta and Krishnamurthy, 2005; John et al., 2019).

An important prerequisite for optimizing this process involves finding quantitative relationships between the leaching yield and the technological parameters. Generally, parameters affecting the leaching of RE concentrates are as follows: (1) the acid/concentration mass ratio parameter (the variable group representing the composition of the concentrate) and (2) the leaching parameters (the variable group representing the mineralogical features of the concentrate) (Jha et al., 2016; Gupta and Krishnamurthy, 2005; John et al., 2019). Traditionally, optimization in chemical engineering has been performed by analyzing the influence of one factor on an experimental response while only one parameter is changed and the others are kept constant. This optimization technique is known as a single-variable optimization design. Its major drawback is that it does not include the interactive effects among the variables studied. Consequently, this technique fails to identify the complete effects of the parameter on the response (Bezerra et al., 2008; Anderson and Whitcomb, 2016). Single-variable optimization increases the number of experiments required to conduct the research; this leads to an increase in time taken, incurred expenses, and consumption of reagents and materials. To overcome this problem, the response surface methodology (RSM) has attracted considerable attention as a collection of mathematical and statistical techniques that can be used for analyzing the effects of several independent variables and for assessing the relationships among the response values and the independent variables. The theory and steps for the application of RSM were detailed by Bezerra et al. (2008) and Anderson and Whitcomb (2016). In comparison with the traditional methods, RSM offers many advantages: it is more economical, it requires a lower number of experiments, it studies the interactions among the parameters and response, it predicts the response, and it checks the adequacy of the method (Hung et al., 2017, 2018; Bezerra et al., 2008; Anderson and Whitcomb, 2016). When a response or a set of responses of interest are influenced by several variables, RSM can be applied effectively. The objective is to simultaneously optimize the levels of these variables to achieve the best system performance. The successful application of RSM to study optimization in chemical-engineering has been well documented (Hung et al., 2017, 2018; Ha et al., 2014; Haldorai et al., 2015; Chen et al., 2012; Jain et al., 2011; Iqbal et al., 2016; Mourabet et al., 2017, 2015; Rodrigues et al., 2012). To the best of our knowledge, no study has been conducted based on the leaching of RE concentrate using RSM. In this study, the RSM based on CCF design was empirically use to study and model the interactive effects of the technological parameters (independent variables) on RE recovery (dependent response). The leaching temperature, acid/conc. Mass ratio, and leaching time were selected as the three main influential factors, and the leaching yield was the response value (Hung et al., 2017, 2018). Finally, the leaching process was optimized using the regression model.

The Yen Phu mine is located in the Yen Phu village, Van Yen district, Yen Bai province, Vietnam; it is approximately 200 km away from Hanoi as shown in Fig. 1; it is one of the four highly promising RE mining locations in Vietnam; the others include Dong Pao and Nam Xe (bastnaesite), and Muong Hum (monazite) as shown in Fig. 1. Yen Phu mine is rich in high-value commercial RE metals such as Neodymium (Nd) and especially Dysprosium (Dy), Terbium (Tb), and Yttrium (Y); the total RE_2O_3 reserves of the Yen Phu mine is approximately 31,700 metric tons with 900 metric tons, 300 metric tons, and 7000 metric tons of Dy, Tb, and Y metal reserves, respectively. Additionally, the mine is relatively rich in niobium ore; but the high radioactivity of the ore is a drawback. Therefore, studies based on the comprehensive processing of Yen Phu xenotime concentrate to produce commercially feasible RE

Table 1 The compositions of Yen Phu xenotime concentrate.

S·N	RE metals	Concentration content,in %	RE content, in %	S·N	Other metals	Concentration content, in %
1	La	1.41	8.70	1	Fe	9.54
2	Ce	2.85	17.58	2	Si	13.29
3	Pr	0.20	1.23	3	Al	1.50
4	Nd	2.72	16.78	4	Mn	0.19
5	Sm	0.53	3.27	5	K	0.14
6	Eu	0.06	0.37	6	Na	0.07
7	Gd	0.65	4.01	7	Ti	0.15
8	Tb	0.04	0.25	8	Mg	6.00
9	Dy	0.87	5.37	9	Ca	1.00
10	Ho	0.06	0.37	10	Cu	0.10
11	Er	0.77	4.75	11	Ta	0.002
12	Tm	0.19	1.17	12	Nb	0.05
13	Yb	0.43	2.65	13	Th	0.17
14	Lu	0.06	0.37	14	U	0.04
15	Y	5.37	33.13			
Total RE metals		16.21	100			
Total RE oxides		19.42	100			

S·N is serial number.

metals are important.

In this study, the modeling of sulfuric acid leaching of Yen Phu xenotime concentrate was reported for optimizing the process. Shrinking core models for spherical particles of constant size based on the Arrhenius equation are empirically used to study the kinetics of leaching the Yen Phu xenotime concentrate. The leaching rate dependence upon time at the leaching temperatures are calculated from the CCF model and experimentally retested. The obtained data are used to calculate the activation energies of the leaching based on kinetic models of the chemical reaction stage or diffusion stage. The leaching mechanism described based on the calculated activation energies and leaching rate is also discussed to optimize the leaching parameters.

2. Materials and methods

2.1. Materials

The Yen Phu xenotime concentrate was supplied by Sunny Group Joint-stock Company (the company that owns the Yen Phu mine). The element content in the concentrate is presented in Table 1. The sulfuric acid consumption required for leaching the concentrate was theoretically calculated from the RE metal content and other contents in the concentrate as shown in Table 1. From Table 1, the acid mass to sulfatize RE metals and other contents in 100 g of the concentrate were ~20 g and ~77 g of concentrated (98%) sulfuric acid, respectively. Thus, the theoretic acid/conc. Mass ratio was approximately 1.

Table 3 Estimated regression coefficients for sequential model.

Source	Coefficient	Standard error	p-value
Model	96.3818	0.46125	1.55E-19
X_1	−11.82	0.424289	8.24E-11
X_2	5.03999	0.424289	3.21E-07
X_3	1.51	0.424289	0.005191
X_1^2	−15.6546	0.809087	2.97E-09
X_2^2	−4.55453	0.809087	0.000219
X_3^2	−1.60455	0.809087	0.075475
X_1X_2	0.4875	0.474369	0.328316
X_1X_3	−1.2375	0.474369	0.026098
X_2X_3	0.937495	0.474369	0.076341

Various characteristics of the original and processed concentrates were examined by the scanning electron microscope (SEM) method for particle morphology and the laser scattering method for particle size distribution. The micrograph of the original concentrate, as shown in Fig. 2 (A), shows that particles of the original concentrate are spherical in shape. The particle size distribution of the original concentrate is shown in Fig. 2 (B).

Concentrated (98%) sulfuric acid of analytical purity was used to study the modeling and kinetic of the concentrate leaching.

2.2. Experiments

The study based on Yen Phu xenotime concentrate leaching was conducted in a rotary tube furnace (Nabertherm, Germany) as shown in Fig. 3 (A); and the rotational speed was fixed at 6 rpm (rpm), which was obtained from our preliminary experiments of the effect of rotational speed on the leaching yield. Experiments were performed at a laboratory scale; a total of 1000 g of dry concentrate was considered for each experiment. Five replications for each experiment were performed. A

Table 2 Central composite rotatable design arrangement and results.

Run	Independent variables						Responses	
	Coded levels			Real values			Experimental* (Actual),in %	Calculated(Predicted),in %
	X_1	X_2	X_3	Leaching temperature,in °C	Acid/conc. Mass ratio,in wt./wt.	Leaching time, in h		
1	−1	−1	−1	250	0.8	2	78.6	80.0
2	1	−1	-1	450	0.8	2	58.3	55.4
3	-1	1	-1	250	1.8	2	88.1	87.3
4	1	1	-1	450	1.8	2	66.9	67.1
5	-1	-1	1	250	0.8	6	83.7	83.6
6	1	-1	1	450	0.8	6	55.6	56.6
7	-1	1	1	250	1.8	6	94.1	94.6
8	1	1	1	450	1.8	6	70.8	69.5
9	-1	0	0	250	1.3	4	93.6	92.5
10	1	0	0	450	1.3	4	68.3	68.9
11	0	-1	0	350	0.8	4	88.7	86.8
12	0	1	0	350	1.8	4	95.4	96.9
13	0	0	-1	350	1.3	2	93.6	93.3
14	0	0	1	350	1.3	6	96.4	96.3
15	0	0	0	350	1.3	4	97.2	96.4
16	0	0	0	350	1.3	4	94.8	96.4
17	0	0	0	350	1.3	4	95.3	96.4
18	0	0	0	350	1.3	4	96.9	96.4
19	0	0	0	350	1.3	4	96.7	96.4
20	0	0	0	350	1.3	4	96.5	96.4

*Experimental mean of five replications per batch.

Table 4 Data obtained from $1-(1-\eta)^{\frac{1}{3}} = k_c t$.

Parameters	473 K (200 °C)	513 K (240 °C)	553 K (280 °C)	593 K (320 °C)
k_c, in s^{-1}	5E-06	7E-06	1E-05	1E-05
R^2	0.9896	0.9898	0.9918	0.9959

Table 5 Data obtained from $1-3(1-\eta)^{\frac{2}{3}} + 2(1-\eta) = k_d t$.

Parameters	473 K (200 °C)	513 K (240 °C)	553 K (280 °C)	593 K (320 °C)
k_d, in s^{-1}	7E-06	1E-05	2E-05	2E-05
R^2	0.9917	0.9962	0.9938	0.9940

Table 6 The predicted yields of the concentrate at various acid/conc. Mass ratios and leaching times (the leaching temperature of 320 °C).

Acid/conc. Mass ratio	Yields, in %				
	3 h	3.5 h	4 h	4.5 h	5 h
1.2	96.1	96.9	97.4	97.7	97.8
1.3	97.2	98.0	98.5	98.9	99.1
1.4	97.9	98.9	99.3	99.7	99.9
1.5	98.2	99.3	99.7	100	100
1.6	98.2	99.3	99.8	100	100

procedure for each leaching experiment was as follows:

i. Sample preparation: A dry concentrate of 1000 g and a given weight of concentrated (98%) sulfuric acid of analytical purity were placed in a ceramic tube with an inner diameter of 90 mm and a length of 500 mm as shown in Fig. 3 (B). After the mixture was mixed for 2 h using a laboratory self-made mixer in a fume hood, the tube was placed in the rotary tube furnace.

ii. Leaching of the concentrate: The leaching process was conducted at temperatures of 200–650 °C, acid/conc. Mass ratios of 0.8–1.8 for 2–6 h. After the completion of the leaching experiment, the leached concentrate was dissolved in deionized water then kept for 2 h at room temperature. Subsequently, the solid-liquid mixture was filtrated and washed. The RE sulfate supernatant and solid residue (the processed concentrate) were collected separately.

iii. Analysis of the REs: RE contents in the RE sulfate solution and the solid residue as well as in the concentrate were determined by the inductive coupled plasma optical emission spectrometer (ICP-OES, Horiba, Japan). The leaching yield (or the leaching rate) of the concentrate was calculated from the total RE contents in the original (initial) concentrate and in the solid residue after leaching as follows:

$$\text{Leaching yield (\%)} = \frac{\text{Initial total REs} - \text{Total REs in residue}}{\text{Initial total REs}} \times 100$$

A satisfactory mass balance was obtained for each leaching experiment.

The morphologies and particle size distributions of the original and processed concentrate particles were analyzed by the SEM (JEOL-IT100LV, Horiba, Japan) and laser scattering (PARTICA LA-960, Horiba, Japan) methods.

2.3. Modeling

Method of modeling and statistical design of experiments on a CCF design (in RSM) improved by Box and Hunter was empirically used (Hung et al., 2017, 2018) for modeling the Yen Phu xenotime concentrate leaching. The leaching yield (Y, %) was considered the dependent response, and the leaching temperature (X_1, °C), acid/conc. Mass ratio (X_2, wt./wt.), and leaching time (X_3, h) were considered independent variables (factors). The variables' levels in coded and actual values are presented in Table 2. The total number of required experimental runs was $2^k + 2k + n_0 = 20$, where k is the number of factors (k = 3) and n_0 is the number of replications at the center points ($n_0 = 6$). Experimental matrix in the planning experimental region is also presented in Table 2. The experimental results were also entered into the MODDE 5.0 software to fit the model by multiple linear regressions. The CCF regression model can be described in the form given in Eq. (6).

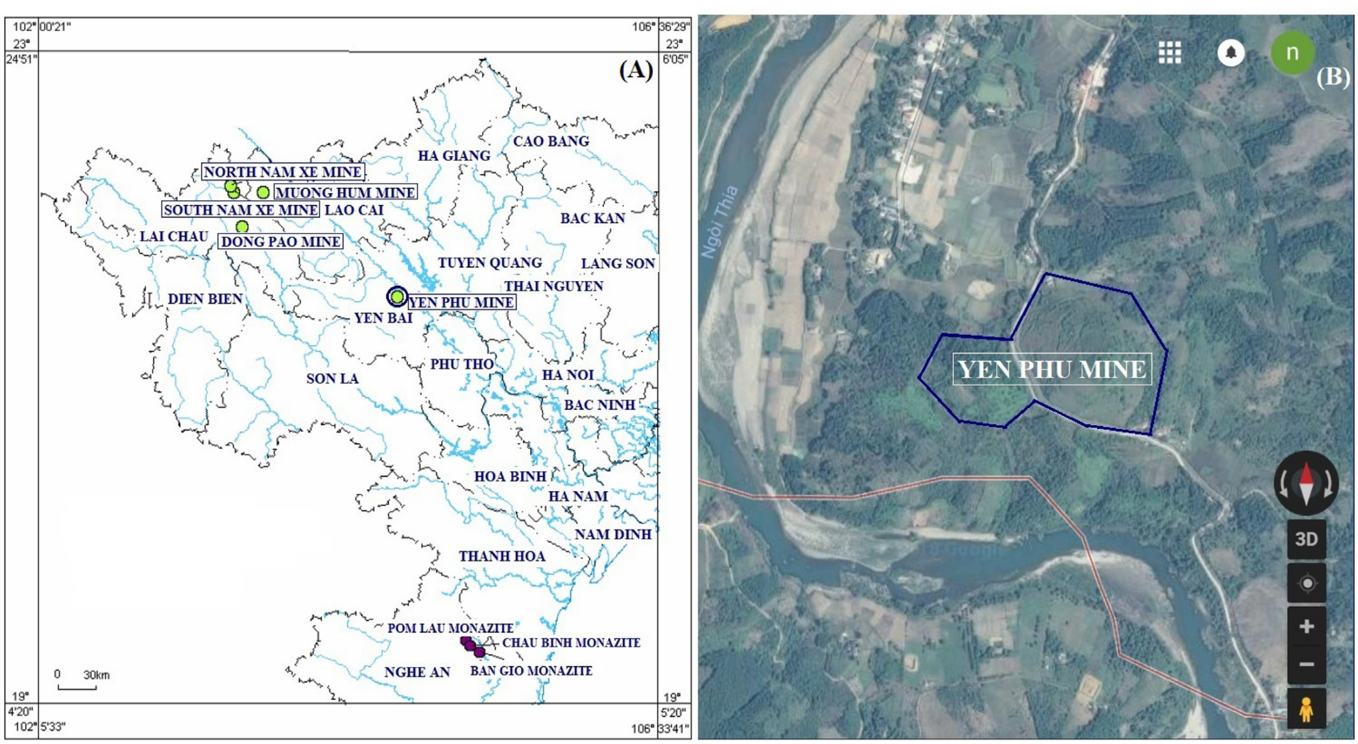

Fig. 1. The RE mines in Vietnam (A) and the google map of Yen Phu mine (B).

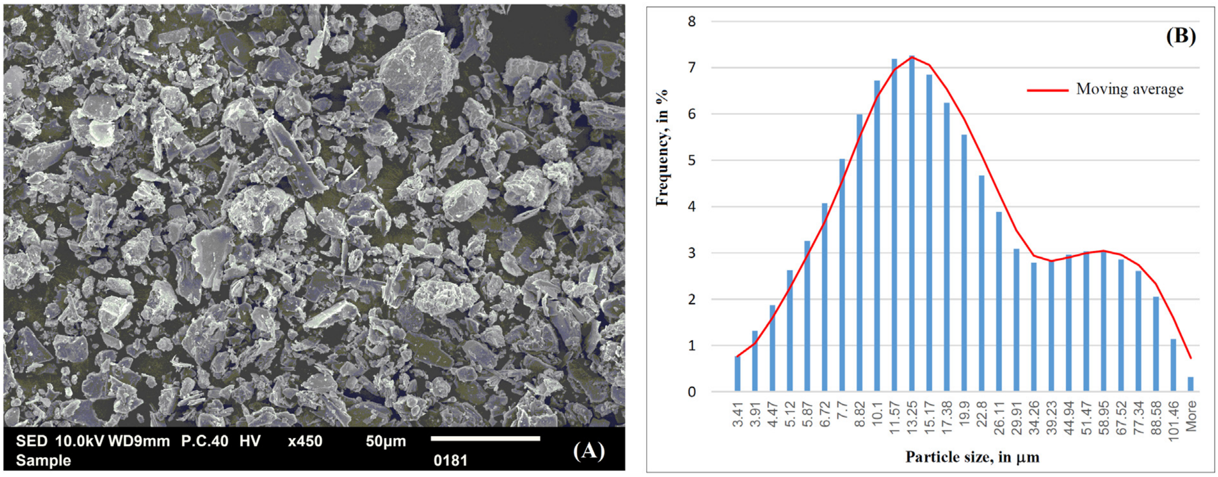

Fig. 2. The SEM photograph (A) and particle size distribution (B) of the original concentrate.

$$Y = b_0 + \sum_{i=1}^{k} b_i X_i + \sum_{i=1}^{k} b_{ii} X_i^2 + \sum_{i,j=1(i \neq j)}^{k} b_{ij} X_i X_j \tag{6}$$

where,Y is the dependent response;b0 is the constant coefficient;bi, bii and bij are the linear, quadratic, and interaction coefficients, respectively;Xi and Xj are the coded values of the independent variables;XiXj and X_i^2 represent the interaction and quadratic terms, respectively.

The analyses of variance (ANOVA) and response surface plots were performed using the MODDE software (version 5.0, Umetrics Inc., Sweden). The optimum conditions were estimated through regression analysis and response surface plots of the independent variables and each dependent response.

For studying the kinetics of Yen Phu xenotime concentrate leaching, the shrinking core models for spherical particles of constant size based on the Arrhenius equation were empirically used. The data of the leaching rate dependence upon time at the leaching temperatures were calculated from the CCF model and experimentally retested. The data were entered into the kinetic models of the chemical reaction stage or diffusion stage to calculate the activation energies of the leaching. The leaching mechanisms are described based on the calculated activation energies and leaching rate versus time plots at the leaching temperatures.

3. Results and discussions

3.1. Determining the planning experimental region

A CCF design in RSM can model the linear, quadratic, and interaction effects of the independent variables on the dependent response; so, a model based on the CCF design would help in accurately describing the overall leaching. Before using the CCF design in RSM to model the leaching, experimental studies based on the effects of the independent variables on the dependent response must be performed to determine a planning experimental region.

The studies based on the effects of temperature on leaching yield were conducted at a fixed acid/conc. Mass ratio of 1.4 and leaching time of 2 h. The results indicated that the leaching yields of the

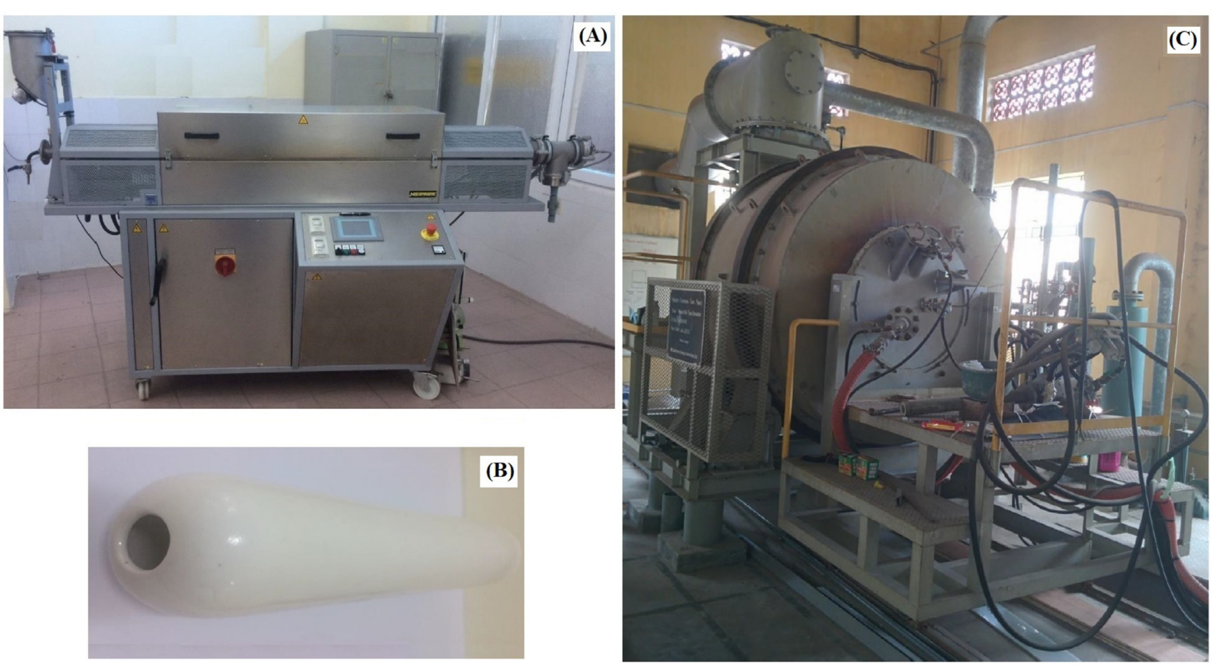

Fig. 3. The rotary tube furnace (A), the ceramic rotary tube (B) and the rotary furnace test plant (C).

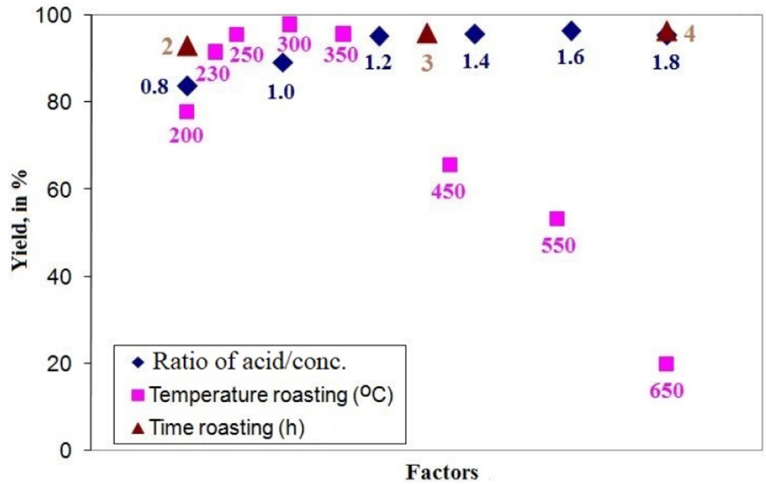

Fig. 4. The effects of factors on the leaching yield of the concentrate.

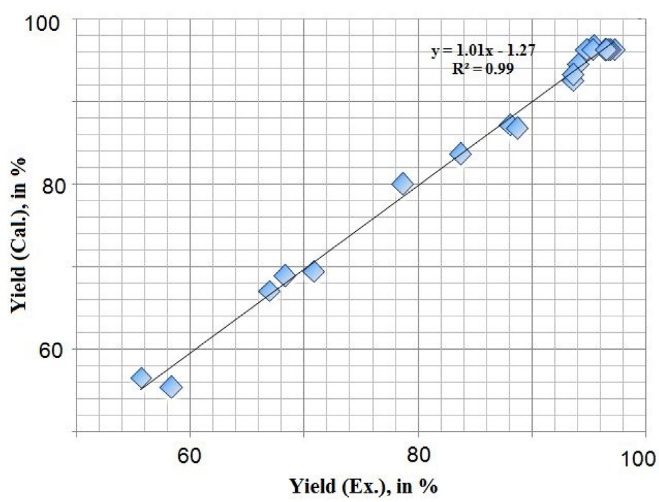

Fig. 5. Linear correlation between calculated and experimental values for the leaching of the concentrate.

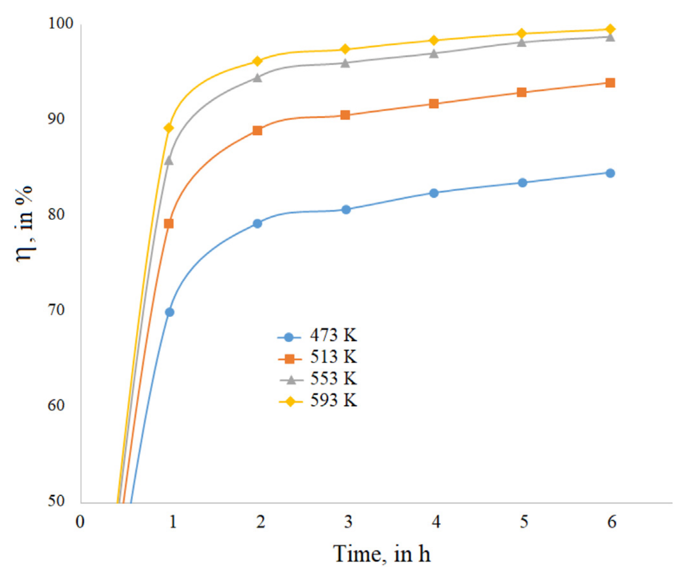

Fig. 7. Plot of the leaching percent rate vs. time at the leaching temperatures (the acid/conc. Mass ratio of 1.3).

concentrate at temperatures of 200 °C, 230 °C, 250 °C and 300 °C increased by 77.9 ± 1.1%, 91.5 ± 1.9%, 95.6 ± 0.8%, and 97.9 ± 0.4%, respectively; however, at temperatures of 350 °C, 450 °C, 550 °C and 650 °C, the leaching yields decreased by 95.6 ± 0.9%, 65.6%, 53.2%, and 19.9%, respectively. Thus, the leaching yields reach the maximum values at temperatures of 250–300 °C and decrease as the temperature exceeds the range.

The studies based on the effects of acid/conc. Mass ratios on the

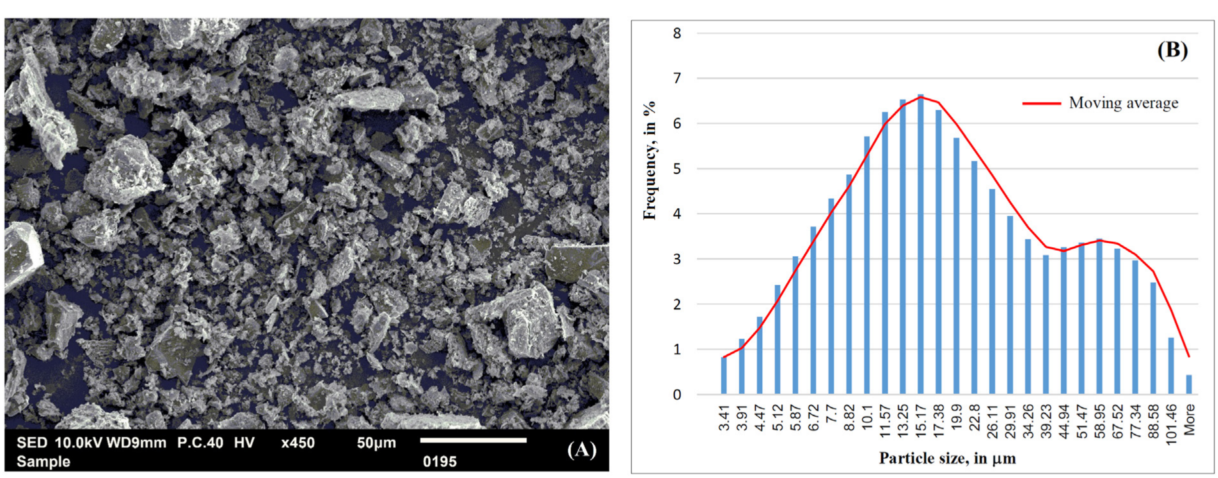

Fig. 6. The SEM photograph (A) and particle size distribution (B) of the processed concentrate.

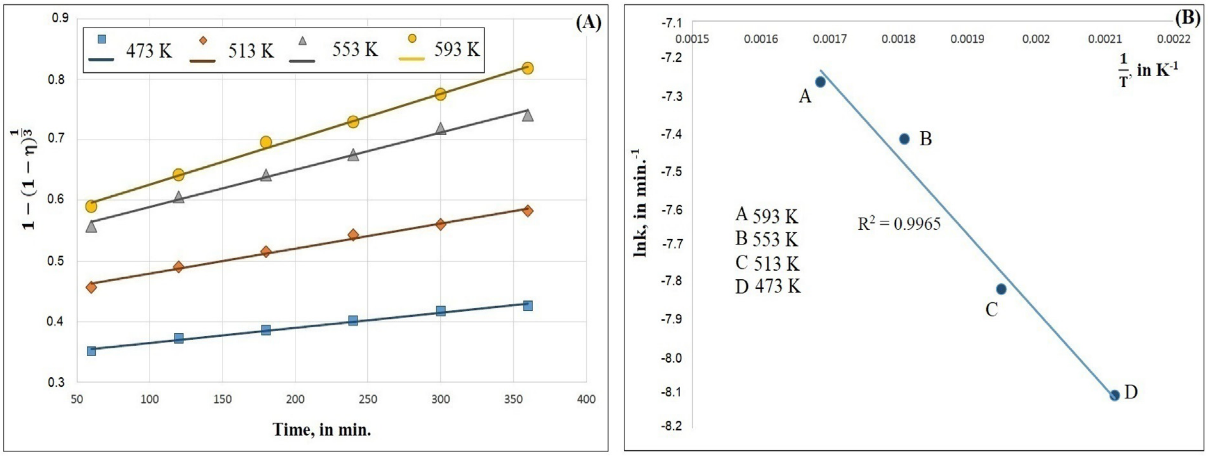

Fig. 8. Plot of $1-(1-\eta)^{\frac{1}{3}}$ vs. time at various temperatures (A) and the Arrhenius plot of chemical reaction stage (B).

leaching yield were conducted at a fixed leaching temperature of 250 °C and leaching time of 2 h. The results indicated that the leaching yields of the concentrate at acid/conc. Mass ratios of 0.8, 1.0, 1.2, 1.4, 1.6, and 1.8 were 83.7 ± 0.5%, 89.3 ± 0.5%, 95.2 ± 1.0%, 95.7 ± 0.8%, 96.4 ± 0.3%, and 95.5 ± 0.3%, respectively. Thus, the leaching yields reach maximum values at ratios of 1.2–1.4 and remain unchanged at the ratios exceeding 1.4.

The studies based on the effects of leaching times on the leaching yield were conducted at fixed acid/conc. Mass ratios of 1.2–1.4 and leaching temperature of 250 °C. The results indicated that the leaching yields of the concentrate at time spans of 2 h, 3 h, and 4 h were 92.9 ± 1.8%, 95.9 ± 1.6%, and 96.4 ± 1.4%, respectively. Thus, the leaching yields reach maximum values at the time span of 3–4 h.

The studies based on the effect of leaching temperature, acid/conc. Mass ratio, and leaching time on the leaching yield of Yen Phu xenotime concentrate are shown in Fig. 4. From the results, the planned experimental region was determined as follows: leaching temperatures 250–450 °C, acid/conc. Mass ratios 0.8–1.8, and leaching times 2–6 h; and the experimental studies for the modeling the leaching were conducted in this planned experimental region.

3.2. Modeling the leaching of Yen Phu xenotime concentrate

The effects of the independent variables, namely leaching temperature 250–450 °C, acid/conc. Mass ratio 0.8–1.8, and leaching time 2–6 h, on the dependent response, namely the leaching yield of Yen Phu xenotime concentrate, were studied based on a CCF design. The quadratic model coded as Y for the leaching yield of the concentrate was selected as suggested by the MODDE 5.0 software. The independent variables in the CCF model (leaching temperature, acid/conc. Mass ratio, and leaching time) were coded as X_1, X_2, and X_3, respectively; the high, center and low levels of X_i are 1, 0 and − 1, respectively, as shown in Table 2. The results of 20 experimental runs are presented in Table 2. The results were also entered into the MODDE 5.0 software to fit the model by multiple linear regressions.

To check the adequacy of the quadratic model, a significance test and ANOVA were employed for the leaching of the concentrate. All estimated regression coefficients and their 95% confidence intervals of model fitting are summarized in Table 3. The probability values (*p*-values) of b_3^2 (of X_3^2), b_{12} (of X_1X_2), and b_{23} (of X_2X_3) coefficients (underlined numbers in Table 3) were greater than 0.05, thereby indicating insignificant confidence levels; hence, they were rejected. The accuracy and variability of the above model can be evaluated by the coefficient of determination (R^2), and it was calculated to be 0.99, thereby showing that the variability of the response is at a 99% confidence level, and the model fails to explain only 1% of the total variation. The results of ANOVA consisting of p-value, sum of square, mean square, model significance (F-value), and degree of freedom show that the p-value for the regression model was less than 0.05, thereby indicating that the model terms were significant at 95% confidence level; thus, the model is statistically good. The p-value of the lack of fit implies that the probability of lack of fit is not significant at the 0.05% level. Statistically, the model has no lack of fit.

The calculated versus experimental plot for the leaching yield of the

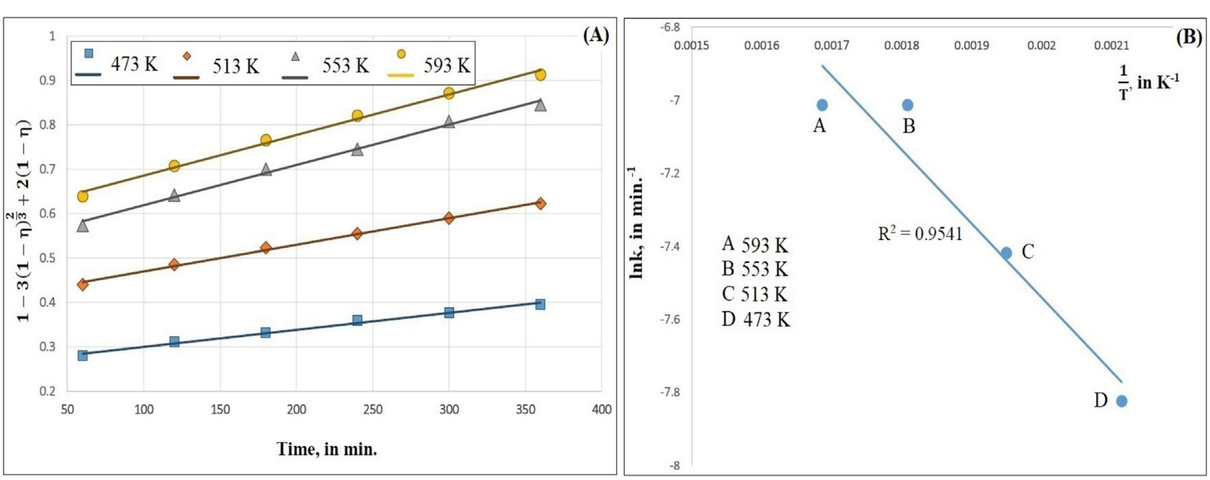

Fig. 9. Plot of $1-3(1-\eta)^{\frac{2}{3}}+2(1-\eta)$ vs. the time at the various temperatures (A) and the Arrhenius plot of diffusion stage (B).

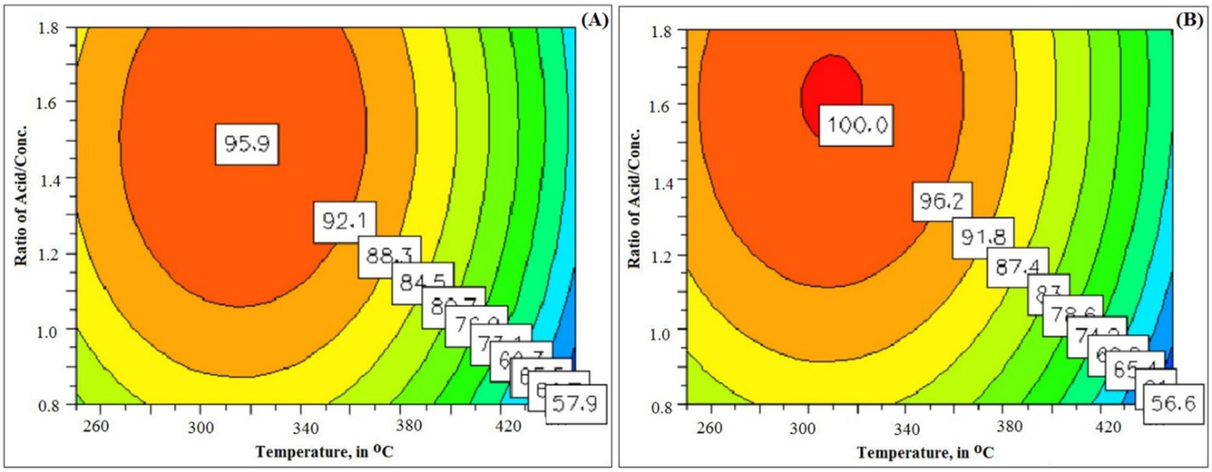

Fig. 10. Contours of the leaching temperature vs. the acid/conc. Mass ratio on the leaching yield of Yen Phu xenotime concentrate at 2 h (A) and at 6 h level of the leaching times (B).

concentrate is shown in Fig. 5. It shows that the experimental results are distributed relatively close to a straight line; and there is a good agreement between the calculated (predicted) and experimental (actual) results. Thus, the CCF model for the leaching of the concentrate is consistent with the experimental data. The final calculated equation for the leaching yield of Yen Phu xenotime concentrate that incorporates the coded coefficients is.

$$Y(\%) = 96.4–11.8\times{}_1 + 5.0\times{}_2 + 1.5\times{}_3–15.7X_1^2–4.6X_2^2–1.\ 2X_1X_3 \quad (7)$$

3.3. Calculating the kinetics of Yen Phu xenotime concentrate leaching

A study based on the kinetics of any chemical reaction is an essential part of designing a chemical process. Most leaching processes are reactions between liquid and solid phases. The Yen Phu xenotime concentrate leaching system includes the concentrate in a solid phase and sulfuric acid in a liquid phase. The micrograph of the original concentrate in Fig. 2 (A) shows that the solid phase characteristics are spherical. Consequently, it was suggested that the kinetic study of concentrate leaching by sulfuric acid can be used for shrinking core models (Levenspiel, 2003; Schmidt, 2005). The successful application of a shrinking core model for spherical particles of constant size to the kinetics of RE leaching by sulfuric acid has been well documented (Jha et al., 2013, 2012; Kim et al., 2014; Feng et al., 2013; Li et al., 2013, 2017; Huang et al., 2017). On the other hand, the SEM photographs of the original and processed concentrate as shown in Figs. 2 (A) and 6 (A) show spherical particles, and the particle size distributions of the original and processed concentrates as shown in Figs. 2 (B) and 6 (B) maintained the same approximate size after the leaching reaction. Thus, the kinetics of Yen Phu xenotime concentrate leaching was analyzed using the shrinking core models for spherical particles of constant size (Jha et al., 2013, 2012; Kim et al., 2014). Generally, the leaching kinetics were described by a two-stage model of a chemical reaction, followed by a diffusion stage (Jha et al., 2013, 2012; Kim et al., 2014; Feng et al., 2013; Li et al., 2013, 2017; Huang et al., 2017). The kinetic model for the chemical reaction stage may be expressed as follows (Jha et al., 2013, 2012; Kim et al., 2014):

$$1-(1-\eta)^{\frac{1}{3}} = k_c t, \quad (8)$$

where η (%) is the leaching rate of the concentrate, k_c (s^{-1}) represents the rate constant of the chemical reaction stage, and t (s) is the reaction time.

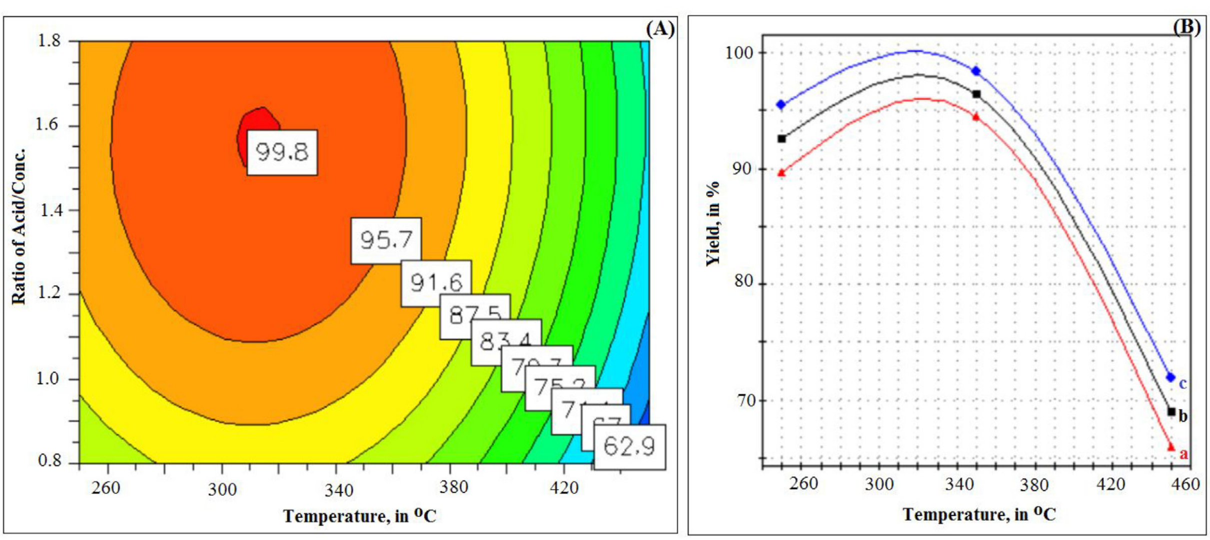

Fig. 11. Contours of the leaching temperature vs. the acid/conc. Mass ratio on the leaching yield of Yen Phu xenotime concentrate at 4 h level of the leaching time (A) and predictive plot that shown the effect of the leaching temperature on the leaching yield of Yen Phu xenotime concentrate at the center level of the acid/conc. Mass ratio and the leaching times of 2 h (a), 4 h (b), 6 h (c) (B).

For diffusion-controlled reactions, there are many kinetic models (Dickinson and Heal, 1999; Órfão and Martins, 2002). The reaction rate can be expressed in terms of the diffusion rate of sulfuric acid through the layers as shown in Eq. (9) (Jha et al., 2013; Kim et al., 2014):

$$1 - 3(1 - \eta)^{\frac{2}{3}} + 2(1 - \eta) = k_d t \quad (9)$$

where k_d in s^{-1} represents the rate constant of the diffusion stage.

The CCF model, represented by Eq. (7), indicated that the temperature range for concentrate leaching must be from 473 K (200 °C) to 593 K (320 °C). Therefore, the study based on the kinetics of leaching was conducted for this temperature range, and the leaching rate data of the concentrate dependence upon time at the leaching temperatures were calculated by the CCF model represented by Eq. (7). The data were experimentally retested and then fitted into the kinetic model for the chemical reaction stage and the diffusion stage according to Eq. (8) and Eq. (9), respectively. Fig. 7 presents the leaching rate of the Yen Phu xenotime concentrate versus time at leaching temperature range of 473–593 K (200–320 °C).

Fig. 8 (A) shows the results that were analyzed by the equation of the interfacial reaction kinetic model, as shown in Eq. (8). Based on this equation, the rate constant (k_c) can be calculated by the least square method at various leaching temperatures as shown in Fig. 8 (A). The data obtained from the regression by Eq. (8) are presented in Table 4.

The kinetic constants presented in Table 4 are derived by Eq. (10) that is also known as the Arrhenius equation, and the results are shown in Fig. 8 (B).

$$\ln k = \ln A - \frac{E}{RT}, \quad (10)$$

where k is the reaction rate constant, A is the frequency factor, R is the gas constant, T is the thermodynamic temperature, and E is the activation energy. The Arrhenius plot of lnk versus $\frac{1}{T}$ is shown in Fig. 8 (B). According to the Arrhenius equation, $-\frac{E}{R}$ is the slope of the straight line in Fig. 8 (B). Hence, the activation energy (E) can be calculated from Fig. 8 (B) and Eq. (10). As a result, in the chemical reaction stage, the activation energy E obtained from the slope shown in Fig. 8 was 17.3 $kJ \cdot mol^{-1}$.

Based on Eq. (9), the rate constants (k_d) were calculated by the least square method as shown in Fig. 9 (A). Data obtained from the regression by Eq. (9) are presented in Table 5. Similarly, in the diffusion stage, the activation energy obtained from the slope shown in Fig. 9 (B) was 17.3 $kJ \cdot mol^{-1}$. Thus, the activation energies calculated by the two kinetic models are the same. They are relatively smaller than those shown in the study based on leaching reaction kinetics of Baotou (China) RE concentrate with concentrated sulfuric acid at low temperatures, wherein the Baotou RE concentrate was a mixture of bastnaesite ($REFCO_3$) and xenotime ($REPO_4$) with the ratio of the concentrations of $REFCO_3$ and $REPO_4$ being in the range 6:4 to 8:2 (Wang et al., 2010). Thus, the activation energy implies that the reaction rate is controlled by a mixed control model for the chemical reaction followed by the diffusion stage at the leaching temperature range of 473 K to 593 K. Fig. 7 shows that the REs in the concentrate are initially leached out after the chemical reaction; then, the leaching rate became slow. Fig. 6 (B) shows that the particle size of the processed concentrate retained the same approximate size after the leaching. This result indicates that the concentrate has layers of reaction products, and they resist the leaching process; consequently, the reaction rate is controlled by diffusion through the layer. Thus, the diffusion of the liquid sulfuric acid reactant through the layer into the solid concentrate core and its reaction with $LnPO_4$ to leach the Yen Phu xenotime concentrate, as in Eq. (1), is the rate-determining step for the leaching. The kinetic study of the leaching suggests technological methods to reduce the influence of this limiting stage, including decreasing the particle size of the concentrate to decrease the volume of the layer and, mixing and heating the leaching to increase diffusion rate.

3.4. Optimizing the Yen Phu xenotime concentrate leaching

Optimizing the leaching of the concentrate that is intended to be applied into a larger scale involves not only finding the best condition for the highest yield, but also considering the trade-off with other importantly consequent factors such as energy consumption, chemical consumption, and further waste treatment. When a predictive model used to describe the process, the variables that appear in the predictive model are required to be able to adjust so as to satisfy the best overall performance, such as cost, yield, profit, etc. From the studies in Section 3.1 and 3.2, the predictive (CCF) model was proposed that exhibited good consistency with the experimental data. The CCF model can help in investigating the interactive effects of the independent variables (leaching temperature, acid ratio, and leaching time) on the dependent response (leaching yield). On the other hand, the studies based on kinetic model (in Section 3.3) can also help in determining the factor that mainly controls the leaching. In these sections, the studies based on modeling and kinetic of the leaching are combined in order to accurately describe the leaching and to find the parameters to be applied, which may satisfy the overall consideration of up-scaling the process.

From proposed CCF model as shown in Eq. (7), to study the interactive relationship among the independent variables and the dependent response, the corresponding contour and response surface plots of the regression model were obtained using the MODDE 5.0 software. The shapes of the response surfaces and contour plots indicate the nature and extent of the interactions of the different components as shown in Figs. 10 and 11. Fig. 11 (A) demonstrates the effects of the leaching temperature (X_1) and acid/conc. Mass ratio (X_2) on the leaching yield of Yen Phu xenotime concentrate for a leaching time of 4 h.

According to Figs. 10 and 11, the leaching yield is highly favored when the leaching temperature is maintained between 250 °C and 320 °C at a given acid/conc. Mass ratio. Additionally, it can be observed that the leaching yield increases initially and reaches a maximum level at the leaching temperature of 320 °C (level of $X_1 = -0.3$); this is a result of the positive effects of the linear coefficient b_1 (of X_1) at the X_1 level of minus, as shown in Eq. (7). Then, the leaching yield decreases at a leaching temperature exceeding 320 °C; this is a result of the negative effects of linear coefficient b_1 (of X_1) at the X_1 level of plus, as shown in Eq. (7). It is clear that the optimum leaching temperature for Yen Phu xenotime concentrate is 320 °C as shown in Figs. 10 and 11. On the other hand, it can also be seen from Eq. (7) that contributions from the linear coefficient b_1 (of X_1) and quadratic coefficient ${b_1}^2$ (of ${X_1}^2$) on Y were calculated at b_0 + 2% at leaching temperatures in the range of 250 °C to 320 °C.

A optimum leaching temperature (X_1) of 320 °C has the level of $X_1 = -0.3$; substituting $X_1 = -0.3$ into Eq. (7) gives.

$$Y\,(\%) = 98.5 + 5.0 \times {}_2 + 1.5 \times {}_3 – 4.6X_2^2 – 0.4 \times {}_3 \quad (11)$$

It can be seen from Eq. (11) that the contributions of the linear coefficient b_2 (of X_2) and quadratic coefficient ${b_2}^2$ (of ${X_2}^2$) on Y were 0.4% at acid/conc. Mass ratios in the range of 1.3 to 1.8. This means that the leaching yield only increases from 98.5% up to 98.9% at acid/conc. Mass ratios from 1.3 to 1.8. It can also be seen from Eq. (11) that the contributions of the linear coefficient b_3 (of X_3) and interaction coefficient b_{13} (of X_1X_3) on Y were 98.5 ± 0.5% at leaching times in the range of 3 h to 5 h. Thus, the effects of acid/conc. Mass ratio and leaching time on the leaching yield are insignificant at the optimum leaching temperature of 320 °C.

The above assessments of the contributions of X_i to Y indicate that the effect of leaching temperature (X_1) on the leaching yield (Y) is the strongest; it is five times higher than that of X_2 on Y and four times higher than that of X_3 on Y. It is suggested that the optimization of leaching is controlled by the leaching temperature. Moreover, the kinetic study provided the same result; the leaching rate (or leaching yield) is also controlled by the leaching temperature.

The leaching yields at the temperature of 320 °C at various acid/conc. Mass ratios and leaching times calculated from Eq. (7) are presented in Table 6. Considering the energy consumption, low chemical consumption, further waste treatment, and better leaching yield, the optimum data from the Yen Phu xenotime concentrate leaching analyzed by the CCF model are as follows: the leaching temperature, acid/conc. Mass ratio, and leaching time are 320 °C, 1.3, and 4 h, respectively.

The optimum data were tested at a pilot scale on 50 kg dry concentrate per batch using a rotary furnace test plant (Rotary kiln type simulator, Japan) as shown in Fig. 3 (C) to further test the promise of the model. The satisfactory results of the testing showed the potential of the model to be applied in commercial leaching operations.

4. Conclusions

The Yen Phu xenotime concentrate leaching was modeled using the RSM based on a CCF design. The proposed CCF model exhibited good consistency with the experimental data. Based on the CCF model, leaching rate data dependence upon time at the leaching temperatures were calculated. The obtained data were then used to determine the activation energy of concentrate leaching using the shrinking core models for spherical particles of a constant size. The resulting activation energies fitted well to a mixed control model of the chemical reaction followed by a diffusion stage. The study of the kinetics suggested the leaching mechanism and technological methods to reduce the influence of the limiting stages. On the other hand, the modeling suggests that the leaching temperature contributes the most to the leaching yield. Considering the energy consumption, chemical consumption, further waste treatment, and leaching yield, the Yen Phu xenotime concentrate leaching parameters were optimized. The proposed CCF model can potentially be applied in commercial leaching after the pilot test; and it can contribute to the development of technologies for the comprehensive processing of Yen Phu xenotime concentrate to produce commercially feasible Nd, Dy, Tb, and Y.

Acknowledgements

Authors would like to acknowledge the financial support from Ministry project (2019-2020): “Study on technology for preparation of Dysprosium metal from the oxide by metallothermic reduction method” (code: DTCB.11/19/VCNXH), VINATOM.

Authors Dr. Nguyen Trong Hung and Dr. Masayuki Watanabe express their sincere gratitude and thanks to the authorities of VAST and Japan Society for the Promotion of Science (JSPS), JAEA. This research was supported by the VAST-JSPS Bilateral Joint Research Projects (2016-2019): “Analysis of rare-earths by femto-second molecular spectroscopy”.

Authors Dr. Jin-Young Lee and Dr. Rajesh Kumar Jyothi express their sincere gratitude and thanks to the authorities of KIGAM funded by the Ministry of Science, ICT, and Future Planning of Korea. This research was supported by the Convergence Research Project (CRC-15-06-KIGAM) funded by the National Research Council of Science and Technology (NST).

References

Anderson, M.J., Whitcomb, P.J., 2016. RSM Simplified: Optimizing Processes Using Response Surface Methods for Design of Experiments, 2nd ed. CRC Press.
Berry, L., Galvin, J., Agarwal, V., Safarzadeh, M.S., 2017. Alkali pug bake process for the decomposition of monazite concentrates. Miner. Eng. 109, 32–41.
Bezerra, M.A., Ricardo, E.S., Oliveira, E.P., Leonardo, S.V., Escaleira, L.A., 2008. Response surface methodology (RSM) as a tool for optimization in analytical chemistry. Talanta 76, 965–977.
Chen, G., Chen, J., Srinivasakannan, C., Peng, J., 2012. Application of response surface methodology for optimization of the synthesis of synthetic rutile from titania slag. Appl. Surf. Sci. 258 (7), 3068–3073.
Dickinson, C.F., Heal, G.R., 1999. Solid-liquid diffusion controlled rate equations. Thermochim. Acta 340–341 (89–103).
El Hady, S.M., Bakry, A.R., Al Shami, A.A.S., Fawzy, M.M., 2016. Processing of the xenotime concentrate of southwestern Sinai via alkali fusion and solvent extraction. Hydrometallurgy 163, 115–119.
Feng, X., Long, Z., Cui, D., Wang, L., Huang, X., Zhang, G., 2013. Kinetics of rare earth leaching from baked ore of bastnaesite with sulfuric acid. Trans. Nonferrous Met. Soc. China 23, 849–854.
Gupta, C.K., Krishnamurthy, N., 2005. Extractive Metallurgy of Rare Earths. CRC Press.
Ha, V.H., Lee, J.C., Hai, H.T., Jeong, J., Pandey, B.D., 2014. Optimizing the thiosulfate leaching of gold from printed circuit boards of discarded mobile phone. Hydrometallurgy 149, 118–126.
Haldorai, Y., Rengaraj, A., Ryu, T., Shin, J., Yun, S.H., Han, Y.K., 2015. Response surface methodology for the optimization of lanthanum removal from an aqueous solution using a Fe_3O_4/chitosan nanocomposite. Mater. Sci. Eng. B 195, 20–29.
Huang, Y., Dou, Z., Zhang, T., Liu, J., 2017. Leaching kinetics of rare earth elements and fluoride from mixed rare earth concentrate after roasting with calcium hydroxide and sodium hydroxide. Hydrometallurgy 173, 15–21.
Hung, N.T., Thuan, L.B., Tung, N.V., Thuy, N.T., Lee, J.Y., Jyothi, R.K., 2017. The UO_2 ex-ADU powder preparation and pellet sintering for optimum efficiency: experimental and modeling studies. J. Nucl. Mater. 496, 177–181.
Hung, N.T., Thuan, L.B., Thanh, T.C., Nhuan, H., Khoai, D.V., Tung, N.V., Lee, J.Y., Jyothi, R.K., 2018. Modeling the UO_2 ex-AUC pellet process and predicting the fuel rod temperature distribution under steady-state operating condition. J. Nucl. Mater. 504, 191–197.
Innocenzi, V., Michelis, I.D., Bernd, K., Vegliò, F., 2014. Yttrium recovery from primary and secondary sources: a review of main hydrometallurgical processes. Waste Manag. 34 (7), 1237–1250.
Iqbal, M., Iqbal, N., Bhattib, I.A., Ahmadb, N., Zahid, M., 2016. Response surface methodology application in optimization of cadmium adsorption by shoe waste: a good option of waste mitigation by waste. Ecol. Eng. 88, 265–275.
Jain, M., Garg, V.K., Kadirvelu, K., 2011. Investigation of Cr(VI) adsorption onto chemically treated *Helianthusannuus*: optimization using response surface methodology. Bioresour. Technol. 102 (2), 600–605.
Jha, M.K., Kumari, A., Choubey, P.K., Lee, J.C., Vinay, K., Jeong, J., 2012. Leaching of lead from solder material of waste printed circuit boards (PCBs). Hydrometallurgy 121–124 (28–34).
Jha, M.K., Kumari, A., Jha, A.K., Vinay, K., Hait, J., Pandey, B.D., 2013. Recovery of lithium and cobalt from waste lithium ion batteries of mobile phone. Waste Manag. 33, 1890–1897.
Jha, M.K., Kumari, A., Panda, R., Jyothi, R.K., Yoo, K., Lee, J.Y., 2016. Review on hydrometallurgical recovery of rare earth metals. Hydrometallurgy 165, 2–26.
John, D., Elizabeth, H., Karin, S., Gamini, S., 2019. The sulfuric acid bake and leach route for processing of rare earth ores and concentrates: a review. Hydrometallurgy 188, 123–139.
Jordens, A., Cheng, Y.P., Waters, K.E., 2013. A review of the beneficiation of rare earth element bearing minerals. Miner. Eng. 41, 97–114.
Kanazawa, Y., Kamitani, M., 2006. Rare earth minerals and resources in the world. J. Alloys Compd. 408–412 (1339–1343).
Kim, C., Yoon, H.S., Chung, K.W., Lee, J.Y., Kim, S.D., Shin, S.M., Lee, S.J., Joe, A.-R., Lee, S.I., Yoo, S.J., Kim, S.H., 2014. Leaching kinetics of lanthanum in sulfuric acid from rare earth element (REE) slag. Hydrometallurgy 146, 133–137.
Kumari, A., Panda, R., Jha, M.K., Joythi, R.K., Lee, J.Y., 2015. Process development to recover rare earth metals from monazite mineral: a review. Miner. Eng. 79, 102–115.
Kuzmin, V.I., Pashkov, G.L., Lomaev, V.G., Voskresenskaya, E.N., Kuzmina, V.N., 2012. Combined approaches for comprehensive processing of rare earth metal ores. Hydrometallurgy 129–130 (1–6).
Levenspiel, O., 2003. Chemical Reaction Engineering, 3rd ed. John Wiley & Sons Inc., New York.
Li, M., Zhang, X., Liu, Z., Hu, Y., Wang, M., Liu, J., Yang, J., 2013. Kinetics of leaching fluoride from mixed rare earth concentrate with hydrochloric acid and aluminum chloride. Hydrometallurgy 140, 71–76.
Li, M., Zhang, D., Yan, Y., Gao, K., Liu, X., Li, J., 2017. Effect of oxidation behavior of cerium during the roasting process on the leaching of mixed rare earth concentrate. Hydrometallurgy 174, 156–166.
Mourabet, M., El Rhilassi, A., El Boujaady, H., Bennani-Ziatni, M., El Hamri, R., Taitai, A., 2015. Removal of fluoride from aqueous solution byadsorption on hydroxyapatite (HAp) using response surface methodology. J. Saudi Chemical Soc. 19, 603–615.
Mourabet, M., El Rhilassi, A., El Boujaady, H., Bennani-Ziatni, M., Taitai, A., 2017. Use of response surface methodology for optimization of fluoride adsorption in an aqueous solution by Brushite. Arab. J. Chem. 10 (2), S3292–S3302.
Órfão, J.J.M., Martins, F.G., 2002. Kinetic analysis of thermogravimetric data obtained under linear temperature programming – a method based on calculations of the temperature integral by interpolation. Thermochim. Acta 390, 195–211.
Pamela, A., Suri, A.K., Gupta, C.K., 1998. Processing of xenotime concentrate. Hydrometallurgy 50, 331–338.
Panda, R., Kumari, A., Jha, M.K., Hait, J., Vinay, K., Jyothi, R.K., Lee, J.Y., 2014. Leaching of rare earth metals (REMs) from Korean monazite concentrate. J. Ind. Eng. Chem. 20, 2035–2042.
Rodrigues, R.C.L.B., William, R.K., Dietrich, D., Thomas, W.J., 2012. Response surface methodology (RSM) to evaluate moisture effects on corn stoverin recovering xylose by DEO hydrolysis. Bioresour. Technol. 108, 134–139.
Sadri, F., Nazari, A.M., Ghahreman, A., 2017a. A review on the cracking, baking and leaching processes of rare earth element concentrates. J. Rare Earths 35 (8), 739–752.
Sadri, F., Rashchi, F., Amini, A., 2017b. Hydrometallurgical digestion and leaching of Iranian monazite concentrate containing rare earth elements Th, Ce, La and Nd. Int. J. Miner. Process. 159, 7–15.

Schmidt, L.D., 2005. The Engineering of Chemical Reactions, 2nd ed. Oxford University Press.

Vijayalakshmi, R., Mishra, S.L., Grupta, C.K., 2001. Processing of xenotime concentrate by sulphuric acid digestion and selective thorium precipitation for separation of rare earths. Hydrometallurgy 61 (2), 75–80.

Wang, X., Liu, J., Li, M., Fan, H., Yang, Q., 2010. Decomposition reaction kinetics of Baotou RE concentrate with concentratedsulfuric acid at low temperature. Rare Metals 29 (2), 121–125.

Wang, L.S., Huang, X., Yu, Y., Zhao, L., Wang, C., Feng, Z., Cui, D., Long, Z., 2017. Towards cleaner production of rare earth elements from bastnaesite in China. J. Clean. Prod. 165, 231–242.

Xie, F., Zhang, T.A., Dreisinger, D., Doyle, F., 2014. A critical review on solvent extraction of rare earths from aqueous solutions. Miner. Eng. 56, 10–28.

Xu, Y., Liu, H., Meng, Z., Cui, J., Zhao, W., Li, L., 2012. Decomposition of bastnaesite and monazite mixed rare earth minerals calcined by alkali liquid. J. Rare Earths 30 (2), 155.

Yoon, H.S., Kim, C.J., Chung, K.W., Kim, S.D., Lee, J.Y., Jyothi, R.K., 2016. Solvent extraction, separation and recovery of dysprosium (Dy) and neodymium (Nd) from aqueous solutions: waste recycling strategies for permanent magnet processing. Hydrometallurgy 165, 27–43.

Zhu, Z., Pranolo, Y., Cheng, C.Y., 2015. Separation of uranium and thorium from rare earths for rare earth production – A review. Miner. Eng. 77, 185–196.